Spin-Current-Induced Magnetotransport in Co–Cu–Co Nanostructures

Frederick B. Mancoff and Stephen E. Russek

Abstract—We report measurements on sub-100-nm Co–Cu–Co spin-valves with the current perpendicular-to-plane. The giant magnetoresistance versus applied magnetic field shows the switching in individually patterned Co nanomagnets. Spin-transfer from the spin-polarized current to the nanomagnets becomes significant for large currents and small devices. The resistance versus applied current shows spin-transfer effects, including current-induced nanomagnet switching and resistance steps indicative of current-induced magnetic precession.

Index Terms—Giant magnetoresistance (GMR), magnetic films and devices, multilayer films, spin-valves.

I. INTRODUCTION

MAGNETIC heterostructure devices, such as giant magnetoresistance (GMR) spin-valves or tunnel junctions, are used for information storage, magnetic random-access memory, and sensor applications. An applied magnetic field is required to switch the ferromagnets. Recent theories have explored a different method of magnetization control: the spin-transfer torque from a spin-polarized current in a ferromagnetic thin film [1]–[8]. In sufficiently small devices, spin-transfer effects should overwhelm the magnetic field created by the current itself [1]. Spin-transfer has been observed experimentally in systems including nanocontacts [9]–[11], electrodeposited nanowires [12], nanoparticles in tunnel junctions [13], and lithographically patterned current-per-pendicular-to-plane (CPP) nanopillar spin-valves [14]–[16]. Further study of current-induced spin-transfer in magnetic nanostructures is of interest, both to understand the interaction between the spin-polarized current and the magnetic body and to utilize the phenomenon for current-controlled magnetotransport applications.

In this paper, we nanofabricated sub-100-nm CPP Co–Cu–Co spin-valves and used the GMR to detect switching in the patterned nanomagnets. We observe spin-transfer-induced nanomagnet switching in the spin-valves through resistance measurements as a function of current. At large magnetic fields, resistance-versus-current sweeps show abrupt resistance increases interpreted as current-induced precession in the spin-valve nanomagnet.
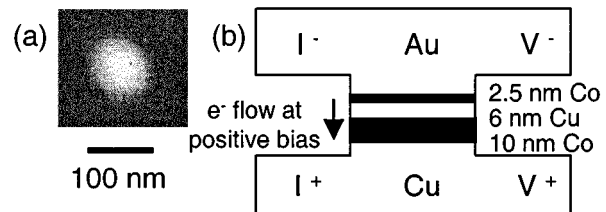
Fig. 1. (a) Scanning-electron micrograph of 80-nm-diameter circular device. (b) Schematic cross section of patterned CPP Co–Cu–Co nanomagnet spin-valve with Au (top electrode) and Cu (bottom electrode).

II. EXPERIMENT

To fabricate the CPP spin-valves, we first sputter-deposited the following thin film onto an oxidized silicon wafer: $Si/SiO_2/5$ nm $Ta/120$ nm $Cu/10$ nm $Co/6$ nm $Cu/2.5$ nm $Co/10$ nm Au. The 5-nm Ta/120-nm Cu serves as a bottom electrode for the active Co–Cu–Co GMR spin-valve, and the 10-nm Au is a passivation layer. Next, we used electron beam lithography and lift off of a thermally evaporated 60-nm Au–50-nm Cr bilayer to form nanosize dots. The Au–Cr dots act as a hard mask for an ion mill step calibrated to etch through the Co–Cu–Co spin-valve and into the bottom Cu electrode, leaving a Co–Cu–Co nanopillar capped with Au with the 50-nm Cr mostly removed. We patterned circular and elliptical nanodots with nominal smallest diameters from 50–200 nm and aspect ratios of 1:1 to 4:1, which varies the spin-valve's shape anisotropy. Fig. 1(a) shows a scanning-electron micrograph of a circular nanostructure with 80-nm diameter. The structure is planarized with insulating polyimide and oxygen plasma etched until the tip of the nanopillar emerges from the polyimide. Photolithography, thermal evaporation, and lift off are used to pattern an Au top contact to the nanopillar. A cross section of the final patterned device is illustrated in Fig. 1(b).

The CPP spin-valve resistance was measured at room temperature and $T = 4$ K while sweeping either the magnetic field or the dc current bias. The dc device resistance R_{dc} was recorded simultaneously with the differential resistance dV/dI from a lock-in amplifier using a small ac current of 50 μA on top of the dc current. As done for Fig. 1(b), we define positive dc current as electron flow from the 2.5-nm Co to the 10-nm Co layer, consistent with the convention of [14].

III. RESULTS AND DISCUSSION

Fig. 2(a) shows a room-temperature lock-in measurement of the device resistance at 0 dc current as a function of in-plane magnetic field. The device is an 80-nm-diameter circular nanopillar, as shown in Fig. 1(a). The data in Fig.
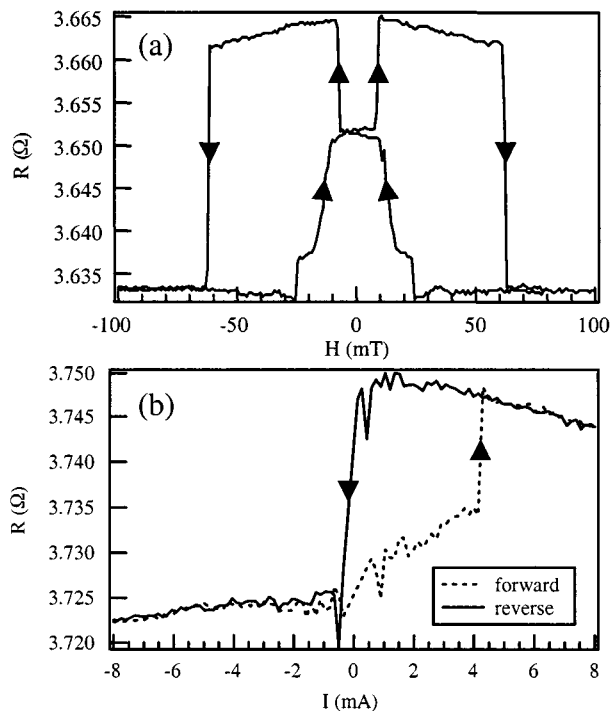
Fig. 2. (a) Room-temperature resistance measured with lock-in amplifier with 0 dc current versus in-plane magnetic field for 80-nm-diameter circular CPP Co–Cu–Co spin-valve shows field-induced GMR. (b) Room-temperature dc resistance versus dc current for same device as in (a) shows current-induced hysteretic switching. Current sweeps from negative to positive (forward, dashed line) and from positive to negative (reverse, solid line).

2(a) are a GMR major loop, showing magnetic-field-induced switching involving both Co layers with a low-resistance parallel-magnetization state at high field and a high-resistance antiparallel-magnetization state at lower field. The GMR acts as a probe to detect relative orientation of the two Co nanomagnetic layers. The maximum change in resistance ΔR for this device is 31 mΩ, which gives $\Delta R/R$ of 0.85%. The arrows in Fig. 2(a) indicate the direction of resistance change during the sweep. Interaction of magnetostatic edge charges for the two Co layers in the nanopillar is expected to favor antiferromagnetic coupling. Starting from the high field in the low-resistance parallel-magnetization state, this antiferromagnetic coupling leads to a reversal to a partially antiparallel state at zero applied field. The multiple resistance plateaus indicate deviation from ideal, single-domain switching for which each Co nanomagnet would have stable directions only parallel or antiparallel to the field. This deviation may be due to micromagnetic defects leading either to multiple domains in each layer or multiple stable magnetization directions.

In addition to the magnetic-field-induced GMR in Fig. 2(a), we also measured room-temperature resistance switching while sweeping the dc current at a constant applied field. Fig. 2(b) shows the measured dc resistance during a current sweep both from positive to negative current (reverse direction, solid line) and from negative to positive current (forward direction, dashed line). To begin, the magnetic field was set to 0.25 T (2.5 kOe) to establish parallel magnetizations and then was reduced, in the case of Fig. 2(b), to 25 mT (250 Oe). The device resistance switched hysteretically, in agreement with previous data

on small CPP spin-valves [14]–[16], including a stable high resistance at positive current and a low resistance at negative current. For the 80-nm device diameter, 1 mA in Fig. 2(b) corresponds to a current density of 2×10^7 A/cm^2.

Due to the difference in thickness between the 2.5-nm and 10-nm Co, the larger moment of the 10-nm layer is expected to remain fixed, relatively undisturbed by spin-transfer torques, while the smaller moment of the 2.5-nm layer can be rotated or reversed by spin-transfer. The constant 25 mT (250 Oe) magnetic field helps fix the 10-nm Co moment direction. As dc current passes through the 10-nm Co layer, the current becomes spin-polarized along the direction of the 10-nm Co magnetization, and the spin-polarized current exerts a spin-transfer torque on the 2.5-nm Co moment. According to [1], spin-transfer from positive current will force the 2.5-nm Co moment antiparallel to the 10-nm Co, and negative current will orient the 2.5-nm Co parallel to the 10-nm Co. This agrees with the asymmetry in Fig. 2(b) with respect to the current polarity. This asymmetry distinguishes spin-transfer from effects due to the Amperian field created by the current, which favors circular vortex magnetizations. Magnetization reorientation by the Amperian field should produce resistance versus current data that are symmetric with respect to current polarity, as no inherent difference exists for the Amperian field with electrons flowing from the 2.5-nm Co to the 10-nm Co or in the opposite direction. Also, the current-induced switching ΔR in Fig. 2(b) is 27 mΩ, comparable to 31 mΩ for field-induced switching [Fig. 2(a)], as evidence that the resistance changes in Fig. 2(b) are due to reorientation of the Co moments. Finally, the switch on the forward (dashed line) sweep in Fig. 2(b) occurs over a range of current, suggesting a process more complicated than a simple single domain switch.

We typically observed the hysteretic current-induced switching events in magnetic fields below 0.1 T (1 kOe). Fig. 3 shows measurements at $T = 4$ K of the dc resistance R_{dc} [Fig. 3(b)] and differential resistance dV/dI [Fig. 3(a)] as a function of dc current, but now with a large in-plane bias field of 0.5–2 T (5–20 kOe). The traces in Fig. 3 for different field values are vertically offset for clarity. The spin-valve in this case is an approximately 250 $\times$80-nm diameter ellipse with the field along the long axis. The upward curve in resistance with increasing current can be attributed to heating, as seen in spin-valves of similar dimensions [14]–[16]. For the current sweeps in Fig. 3, we see critical currents I_{crit} at which an upward spike occurs in dV/dI [Fig. 3(a)] simultaneous with a step increase in R_{dc} [arrows in Fig. 3(b)]. We interpret the data as follows. The large magnetic field should initially set the two Co magnetizations in a low-resistance parallel state. Ramping the current through I_{crit} thus causes a deviation of the Co moments away from the low-resistance parallel state. Such a current-induced resistance increase was observed in both point contacts [9]–[11] and patterned nanopillars [14] and interpreted as indirect evidence for spin-transfer-induced steady-state magnetic precession of the thin 2.5-nm Co. The resulting resistance step in Fig. 3(b) (on top of the background increase from heating) should be a fraction of the device's total field-induced ΔR, as is the case for this spin-valve, for which we observed field-induced ΔR of 6 mΩ at $T = 4$ K.

Fig. 4. Dots show critical currents I_{crit} from Fig. 3(a) versus applied magnetic field. Resistance features in Fig. 3 can be assigned to three critical currents that shift linearly with field. Dashed lines are linear fits for each set.
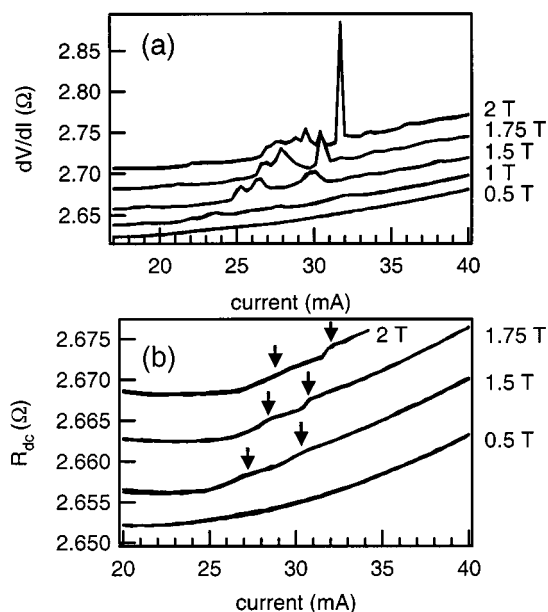
Fig. 3. (a) dV/dI versus dc current at $T = 4$ K for 250 ×80-nm diameter elliptical CPP spin-valve. Data at different magnetic fields are vertically offset for clarity. dV/dI spike positions give critical currents I_{crit}. (b) DC resistance at $T = 4$ K measured simultaneously for the same device. Arrows mark critical currents I_{crit} corresponding to dV/dI spikes in (a).

spin-transfer effects, including current-induced switching and putative magnetic precession. Continued study of these phenomena, particularly with varied spin-valve layer thicknesses, composition, and magnetic anisotropy, as well as high-speed dynamical measurements, should give an increased understanding and control of spin-transfer interactions.

With the 10-nm Co moment fixed by the large applied field, a positive current is expected to produce a spin-transfer torque on the 2.5-nm moment that favors moving away from the parallel magnetization state, producing in this case a precession of the 2.5-nm moment rather than a full reversal as in lower fields. No precessing state is expected at negative currents, for which both the spin-transfer torque and the large field favor parallel Co moments. The expected asymmetry with current polarity for spin-transfer agrees with the observation of spikes and steps in Fig. 3 at positive currents and their absence in our measurements at negative currents. Also, for each field value, we find multiple critical currents, suggesting multiple spin-precessing modes. We have seen multiple critical currents in both our elliptical and circular spin-valves, compared to single critical currents for circular devices in [14].

Fig. 4 summarizes the magnetic field dependence of I_{crit} for the resistance features in Fig. 3. Slonczewski [2] predicts a linear increase with field for the critical current for spin-transfer-induced magnetic precession. Motivated by this, we separate the dV/dI spikes of Fig. 3 into three main features, each with an I_{crit} that increases nearly linearly with field. The dashed lines in Fig. 4 are linear fits for the different spin-precession critical currents. The slopes are between 3.8–5.5 ×10^{-3} A/T (3.8–5.5 ×10^{-7} A/Oe), within a factor of two of the 2.9 ×10^{-3} A/T from similar data on patterned nanopillars [14].

We fabricated sub-100-nm-diameter CPP spin-valves and observed magnetic-field-induced nanomagnet switching as well as
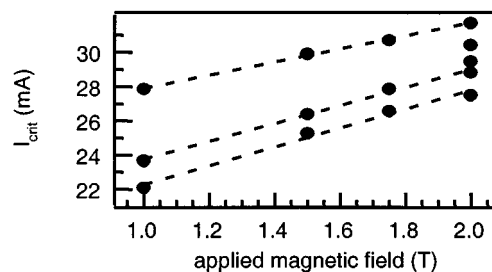
REFERENCES

[1] J. C. Slonczewski, "Current-driven excitation of magnetic multilayers," *J. Magn. Magn. Mater.*, vol. 159, pp. L1–L7, 1996.
[2] ——, "Excitation of spin waves by an electric current," *J. Magn. Magn. Mater.*, vol. 195, pp. L261–L268, 1999.
[3] L. Berger, "Emission of spin waves by a magnetic multilayer traversed by a current," *Phys. Rev. B*, vol. 54, pp. 9353–9358, 1996.
[4] Y. B. Bazaliy, B. A. Jones, and S.-C. Zhang, "Modification of the Landau-Lifshitz equation in the presence of a spin-polarized current in colossal- and giant-magnetoresistive materials," *Phys. Rev. B*, vol. 57, pp. R3213–R3216, 1998.
[5] C. Heide, P. E. Zilberman, and R. J. Elliott, "Current-driven switching of magnetic layers," *Phys. Rev. B*, vol. 63, pp. 064 424/1–064 424/7, 2001.
[6] X. Waintal, E. B. Myers, P. W. Brouwer, and D. C. Ralph, "Role of spin-dependent interface scattering in generating current-induced torques in magnetic multilayers," *Phys. Rev. B*, vol. 62, pp. 12 317–12 327, 2000.
[7] C. Heide, "Effects of spin accumulation in magnetic multilayers," *Phys. Rev. B*, vol. 65, pp. 054 401/1–054 401/17, 2001.
[8] M. D. Stiles and A. Zangwill, "Non-collinear spin transfer in Co/Cu/Co multilayers," *J. Appl. Phys.*, vol. 91, pp. 6812–6817, 2002.
[9] M. Tsoi *et al.*, "Excitation of a magnetic multilayer by an electric current," *Phys. Rev. Lett.*, vol. 80, pp. 4281–4284, 1998.
[10] M. Tsoi *et al.*, "Generation and detection of phase-coherent current-driven magnons in magnetic multilayers," *Nature*, vol. 406, pp. 46–48, 2000.
[11] E. B. Myers *et al.*, "Current-induced switching of domains in magnetic multilayer devices," *Science*, vol. 285, pp. 867–870, 1999.
[12] J.-E. Wegrowe *et al.*, "Current-induced magnetization reversal in magnetic nanowires," *Euro. Phys. Lett.*, vol. 45, pp. 626–632, 1999.
[13] J. Z. Sun, "Current-driven magnetic switching in manganite trilayer junctions," *J. Magn. Magn. Mater.*, vol. 202, pp. 157–162, 1999.
[14] J. A. Katine, F. J. Albert, R. A. Buhrman, E. B. Myers, and D. C. Ralph, "Current-driven magnetization reversal and spin-wave excitation in Co/Cu/Co pillars," *Phys. Rev. Lett.*, vol. 84, pp. 3149–3152, 2000.
[15] F. J. Albert, J. A. Katine, R. A. Buhrman, and D. C. Ralph, "Spin-polarized current switching of a Co thin film nanomagnet," *Appl. Phys. Lett.*, vol. 77, pp. 3809–3811, 2000.
[16] J. Grollier *et al.*, "Spin-polarized current induced switching in Co/Cu/Co pillars," *Appl. Phys. Lett.*, vol. 78, pp. 3663–3665, 2001.